Quantifying the combined effects of pronase and benzalkonium chloride in removing late-stage *Listeria monocytogenes*-*Escherichia coli* dual-species biofilms

Pedro Rodríguez-López[a], Carmen H. Puga[b], Belén Orgaz[b] and Marta L. Cabo[a]*

a. Department of Microbiology and Technology of Marine Products, Instituto de Investigaciones Marinas (IIM-CSIC), Eduardo Cabello 6, 36208 Vigo, Pontevedra, Spain

b. Department of Nutrition, Food Science and Technology. Faculty of Veterinary. University Complutense of Madrid (UCM). Avda. Complutense s/n, 28040 Madrid, Spain.

*Corresponding author: Tel.: +34 986 231 930 E-mail address: marta@iim.csic.es (Marta L. Cabo)

Published in: Rodríguez-López et al. (2017) Biofouling, 33:8, 690-702

DOI: 10.1080/08927014.2017.1356290

Abstract

This work presents the assessment of the effectivity of a pronase (PRN)-benzalkonium chloride (BAC) sequential treatment to remove *Listeria monocytogenes*-*Escherichia coli* dual-species biofilms grown on stainless steel (SS) using fluorescence microscopy and plate count assays.

The effects of PRN-BAC on the occupied area (OA) by undamaged cells in 168 h dual-species samples were determined using a first-order factorial design. Empirical equation obtained significantly (r^2 = 0.927) described a negative individual effect of BAC and a negative interactive effect of PRN-BAC achieving OA reductions up to 46 %. After treatments, high numbers of remaining attached and released *E. coli* viable and cultivable cells were detected in PRN-BAC combinations when low BAC concentrations were used. Therefore, at appropriate BAC doses, in addition to biofilm removal, sequential application of PRN and BAC, represent an appealing strategy for pathogen control in SS surfaces while hindering the dispersion of live cells into the environment.

Keywords

Benzalkonium chloride; Biofilm; Disinfection; Fluorescence microscopy; *Listeria monocytogenes*; Pronase

Introduction

Biofilms are considered the main structure in which bacteria are usually found in the environment (Costerton et al. 1995; Vlamakis 2011; Winkelströter et al. 2013; Abdallah et al. 2014). These structures can be defined as sessile communities of microorganisms residing in a self-secreted matrix (Costerton et al. 1995). Bacteria in this state are able to develop resistance to environmental insults (Davey & O'toole 2000; O'Toole et al. 2000). In the food industry such phenomenon could lead to a higher tolerance to disinfectants (Bridier et al. 2011) causing eventual foodstuffs cross-contamination (Bridier et al. 2015; Muhterem-Uyar et al. 2015).

Listeria monocytogenes is a Gram-positive, environmentally ubiquitous bacterium commonly living in nature in soils rich in plant-decay matter. In humans it can cause listeriosis, a disease with an increasing incidence tendency in Europe over the last years (EFSA 2015). The invasive form of this illness can severely affect newborns, the elderly, pregnant women and individuals with a compromised immune system with symptoms that may vary from septicaemia, neurological harm and miscarriage (Freitag et al. 2009). This pathogen can be also found adhered to surfaces of sanitary and food industrial settings (Gandhi & Chikindas 2007; Rodríguez-López et al. 2015; Zhang et al. 2016). In the latter case, it can persist for long periods of time thus becoming contamination hotspots for food products (Carpentier & Cerf 2011). Besides, this microorganism can easily associate with other bacterial species forming part of complex microbial communities (Carpentier & Chassaing 2004; Rodríguez-López et al. 2015), which can confer higher resistance to biocides (Kostaki et al. 2012; Giaouris et al. 2013).

For biofilm control, chemical-based treatments using peroxides, electrolysed water, organic acids and quaternary ammonium compounds (QACs) have been used alone (McCarthy & Burkhardt 2012; da Silva & De Martinis 2013) or combined (Vázquez-Sánchez et al. 2014) to prevent both formation and remove already formed structures. Among QACs, benzalkonium chloride (BAC) is usually preferred due to its low cost and its bactericidal effects affecting the permeability of the cell membrane and inducing irreversible cell damage (Mcdonnell & Russell 1999; Tezel & Pavlostathis 2015). Nonetheless, in *L. monocytogenes* it has been proved that biofilms present higher resistance to BAC in comparison to the planktonic counterparts (Saá Ibusquiza et al. 2011). This fact has also been observed in Gram-negative species (Houari & Di Martino 2007; Giaouris et al. 2013).

Enzymatic treatments have been proposed as an efficient, environmentally-friendly possibility for surface cleaning as well as a biofilm-preventive strategy in industrial settings (Lequette et al. 2010) or for decontamination of medical devices to prevent infection via indwelling devices (Marion et al. 2006; Stiefel et al. 2016). Since enzymes specifically cleave biological molecules such as proteins, polysaccharides and DNA, they are used to degrade components of the biofilm matrix affecting the stability of the structure and therefore producing an eventual biofilm dispersion (Kaplan 2014). Nevertheless, enzymes used for anti-biofilm procedures in the food industry, generally lack of biocide activity making them inappropriate for bactericidal purposes (Meireles et al. 2016). To overcome this problem, a combination of enzymatic and chemical approaches would be desirable since the action of the enzyme would positively contribute to the killing capacity of the disinfectant (Meireles et al., 2016). With this regard, the study of Kaplan, (2009) demonstrated that DNase I sensitised 24 h *Staphylococcus aureus* biofilms to antiseptics and disinfectants. Besides, a recent study

111 demonstrated that the combination of pronase (PRN) or DNase I with BAC was able to
112 remove 48 h *L. monocytogenes-E. coli* biofilms (Rodríguez-López et al. 2017).

113 For biofilm quantification after disinfection, most of the methods are based on the
114 remaining adhered cells recovered from samples followed by cultivable cells counting
115 on agar plates. However, these agar plating-based techniques present several limitations
116 (Sutton 2011) and they do not provide information regarding morphological features.
117 Therefore, it is usual to incorporate microscopic assays, mainly epifluorescence and
118 confocal laser scanning microscopy (CLSM) for describing 2D and 3D biofilm
119 structures, respectively.

120 In epifluorescence microscopy, an issue of concern is how to select the appropriate 2D
121 parameters for giving an accurate description of the effects, being easily related to
122 biological processes to obtain meaningful conclusions. With this regard, several authors
123 have concluded that the areal porosity, and similar parameters, is a good 2D structural
124 outcome, intuitive, easy to interpret and with clear biological meaning (Christensen et
125 al. 2001; Jackson et al. 2001; Beyenal et al. 2004; Dusane et al. 2008). Beyenal et al.
126 2004 suggested parameter selection according with the specific process under study.
127 Following this criterion, the biological meaning of areal porosity, and by extension the
128 occupied area, seems to be especially adequate to describe biofilm removal.

129 This work aimed to study the effectiveness of combining pronase (PRN) and BAC for
130 the removal of late-stage *L. monocytogenes-E. coli* dual-species biofilms grown on
131 stainless steel (SS), mimicking real industrial conditions where biofilms are formed
132 after long periods. PRN was selected since it has been reported that *L. monocytogenes*
133 biofilm matrix is mainly constituted by proteins (Longhi et al. 2008; Nguyen &
134 Burrows 2014) and is efficient removing early-stage *L. monocytogenes-E. coli* dual-

species biofilms (Rodríguez-López et al. 2017). Enzymes solutions were applied at room temperature to further simulate realistic environmental conditions. The assessment of the effects was performed combining microscopy and image analysis with classical microbiology methods. To ascertain the feasibility of the microscopy approach, the method was firstly statistically evaluated in two different dual-species biofilms: *L. monocytogenes-E. coli* and *L. monocytogenes-Pseudomonas fluorescens*.

Materials and Methods

Bacterial strains

Two different consortia were used. The first was formed by *L. monocytogenes* A1-*E. coli* A14, both isolated from a fish processing plant in a previous survey (Rodríguez-López et al. 2015). The second one was formed by a strain of *L. monocytogenes* G1, isolated from a cheese processing plant, kindly provided by Dr. Luisa Brito (Leite et al. 2006) and *P. fluorescens* B52, as one of the species commonly isolated in dairy industry, was kindly provided by Dr. Carmen San José (Allison et al. 1998). These consortia were chosen based on their relevance in fish and dairy industries, and their capability to form dual-species biofilms. From now on consortia used will be referred as fish industry and dairy industry consortia for A1-A14 and G1-B52 biofilms, respectively.

In all cases, stock cultures were maintained at -80 ºC in Brain-Heart infusion broth (BHI; Biolife, Italy) containing 50% glycerol 1:1 (v v^{-1}) mixed. Laboratory stocks were kept at -20 ºC in Tripticase Soy Broth (TSB; Cultimed, Barcelona, Spain) containing 50% glycerol 1:1 (v v^{-1}) mixed.

Setup of dual-species biofilms

100 µl of laboratory stocks was cultured overnight in 5 ml sterile TSB at 37 ºC for *L. monocytogenes* and *E. coli* and 25 ºC for *P. fluorescens* and subcultured once so as to ensure a proper activation.

Inocula preparation was performed as follows. Briefly, Abs_{700} of cultures was adjusted to 0.1 ± 0.001 in sterile phosphate buffer saline (PBS), corresponding to a bacterial

concentration of about 10^8 CFU ml^{-1} according to previous calibrations. Adjusted cultures were further diluted in sterile mTSB (TSB supplemented with 2.5 g l^{-1} glucose (Vorquímica, S.L., Vigo, Spain) and 0.6 % yeast extract (Cultimed)) until obtaining a final concentration of about 10^4 CFU ml^{-1} and 1:1 (v v^{-1}) mixed.

Biofilms were grown on 10x10x1 mm AISI 316 stainless steel (SS) coupons (Comevisa, Vigo, Spain). Pre-treatment of coupons included individual washing with industrial soap (Sutter Wash, Sutter Ibérica, S.A., Madrid, Spain) to remove grease residues, thoroughly rinsing with tap water with a final rise with deionized water and sterilised by autoclaving them at 121 ºC for 20 min. Coupons were individually placed into a 24 flat-bottomed well plate and each well was inoculated with 1 ml of the corresponding culture. Plates were incubated in a humidified atmosphere at 25 ºC statically for 2 h for initial adhesion, and then in constant shaking at 100 rpm.

In all situations, coupons were aseptically collected and briefly immersed in 1 ml sterile PBS to remove loosely attached cells before any assay was performed.

Plate count assays

In all cases, *Listeria*-PALCAM (Liofilchem, Roseto degli Abruzzi, Italy) was used to select *L. monocytogenes*, Chromogenic *Escherichia coli* agar (Cultimed, Barcelona, Spain) with a supplement of 5 mg l^{-1} of Vancomycin and Cefsulodine (Sigma-Aldrich, St Louis, MO, USA) to isolate *E. coli* and *Pseudomonas* agar base (PAB) with CFC supplement (Liofilchem) for *P. fluorescens*. Plates were incubated for 24-48 h at 37 ºC for Chromogenic agar and PALCAM whereas 25 ºC was preferred for PAB.

200 Attached viable cultivable cells (AVC) were harvested from coupons by scrapping
201 using two sterile cotton swabs moistened in sterile buffered peptone water (BPW).
202 Swabs were then suspended in 2 ml of BPW and vortexed vigorously for 1 min in order
203 to release cells, serially diluted in BPW and spread onto agar plates for AVC
204 determination. In reproducibility, repeatability and biofilm formation kinetics assays
205 AVC values were expressed in CFU cm^{-2} whereas in the enzyme-disinfectant assays
206 they were expressed in log CFU cm^{-2}.

207 Released viable cultivable cells (RVC) into the neutralising solution (preparation
208 detailed later) were determined after treatments performing direct serial dilution of the
209 solution in BPW and spread onto appropriate solid media. Outcomes were expressed in
210 log CFU ml^{-1}.

211

212 ***Fluorescence microscopy and image analysis assays***

213 Samples (SS coupons) were stained for 15 min with FilmTracer™ LIVE/DEAD®
214 Biofilm Viability Kit (Life Technologies, Eugene, OR, USA). Staining solution
215 contained 0.75 µl Syto9 and 0.25 µl propidium iodide in 1 ml of filter sterilised
216 deionised water. Fifty microlitres of this solution were used for each coupon staining
217 and allowed to remain 15 min in the dark. After that, coupons were washed three times
218 in 1 ml of sterile MilliQ water. Coupons were then air dried and visualized in a Leica
219 6000DM (Leica, Wetzlar, Germany) epifluorescence microscope using 10x ocular
220 lenses and 40x objective.

221 From each sample, a randomly chosen field was considered as start point to
222 automatically acquire images using a Leica DFC365 FX camera. Each image set was
223 composed by 3 mosaics of twenty-five 12-bit images covering a total surface of

224 $1.92x10^6$ μm^2. Image analysis was then performed using the Integrated Morphometry
225 Analysis module of the Metamorph MMAF software (Molecular Devices, Sunnyvale,
226 CA, USA) in order to determine the occupied area (OA) by undamaged (green) cells.

227 Results of image analysis in biofilm formation were expressed as the percentage of
228 occupied area (POA) of the mosaic whilst in repeatability, reproducibility and enzyme-
229 disinfectant experiments OA outcomes were expressed in mm^2.

230

231 ***Dual-species biofilm formation kinetics***

232 Samples of both consortia were collected at 24, 48, 72, 96 and 168 h of incubation. In
233 each sampling time, 3 coupons were used for plate count and 3 more for microscopy
234 analysis as described above.

235

236 ***Effects of sequential pronase (PRN) – benzalkonium chloride (BAC) treatments on***
237 ***168 h A1-A14 biofilms***

238 *PRN, BAC and neutralising solution preparation*

239 Pronase (PRN; from *Streptomyces griseus*, Roche, Mannheim, Germany) was prepared
240 at concentrations listed in Table 1 using 0.1 M Tris-HCl (Sigma Aldrich) buffer at pH =
241 7.5 ± 0.2 and then filter sterilised through a 0.2 µm pore diameter syringe filter
242 (Sartorius). Solutions were kept at -20 ºC until use. Benzalkonium chloride (BAC;
243 Guinama, Alboraya, Spain) was prepared at concentrations listed in Table 1 dissolving
244 the stock solution in sterile distilled water according to the concentrations needed, and
245 kept at 4 ºC until use.

Neutralising solution was prepared with following composition per litre: 10 ml of a 34 g l^{-1} KH_2PO_4 solution adjusted to pH = 7.2 with $NaOH_{(aq)}$, 3 g soy lecithin, 5 g $Na_2S_2O_3$, 1 g L-histidine, 30 ml Tween 80 and deionised water (Rodríguez-López et al. 2017). This solution was sterilised by autoclaving at 121 ºC for 20 min and kept at 4 ºC until use.

Experimental design

A first order factorial design (Box 1952; Box et al. 2008) with 4 combinations of variables and 4 replicates in the centre of the domain was carried out. This kind of experimental design provides empirical information about factors without increasing the size of the assay. Besides, it is able to quantify individual and additive effects in a given experimental ambit. The natural values of the independent variables (concentration of PRN and concentration of BAC) were encoded as detailed in Table 1. Maximum and minimum values of each variable were determined in previous experiments (data not shown).

After PBS washing, PRN-BAC combinations (Table 1) were sequentially applied on the 168 h A1-A14 samples. Briefly, 1 ml of each enzymatic solution was applied for 1 h contact time at room temperature, statically. Next, 1.5 ml of the corresponding BAC concentration was allowed to dwell for 10 min at room temperature. Finally, treated coupons were transferred to new wells containing 1 ml of neutralising solution and immersed for 30 s, which was considered the minimum time necessary for proper neutralisation according to a previous assay (data not shown). Untreated biofilm samples were used as controls. Finally, quantification of AVC, RVC and the OA by undamaged cells was carried as described above.

For better understanding, throughout this article the concentrations of the antimicrobial solutions will be displayed as [PRN,BAC] and always expressed in μg ml^{-1}.

Statistical analysis

For the factorial design, least-squares method (quasi-Newton) was used for model fit to experimental data. Significance of the coefficients obtained in the empirical equation was determined by a Student's *t* test ($\alpha = 0.05$). A Fisher test ($\alpha = 0.05$) was employed to test the consistency of the models.

In POA, AVC and RVC determinations, a one-way ANOVA with a *post–hoc* Bonferroni test was used. Significance was expressed at the 95 % confidence level ($\alpha = 0.05$) or greater.

289 **Results**

290 ***Dynamics of dual-species L. monocytogenes biofilm formation***

291 Quantitative characterization of the *L. monocytogenes* mixed biofilms was carried out
292 by combining outputs of OA and plate count assays. First, reproducibility and
293 repeatability of both methods was assessed (supplementary information). In addition to
294 this, the precision of both methods in biofilm formation assays was checked by
295 comparing the coefficients of variation of both methods in each sampling time
296 (supplementary information).

297 In A1-A14 samples, AVC values showed an increasing tendency up to a peak at 72 h of
298 $1.21 \times 10^8 \pm 3.20 \times 10^7$ CFU cm^{-2} followed by a decrease in the last two times of
299 sampling reaching a minimum of about $1.91 \times 10^6 \pm 8.44 \times 10^5$ CFU cm^{-2} at 168 h (Fig.
300 1, Table 2). POA dynamics showed also some fluctuations although not as sharp as in
301 AVC (Fig. 1). Besides, the 72 h peak observed in AVC was not present in POA
302 quantification (Fig. 1).

303 Analysis of the microscopic mosaics showed a clear predominance of undamaged
304 (green-emitting) cells over the sample (Fig. 2). However, green and red cells were
305 equally distributed along the SS surface forming a uniform surface in which cluster
306 formation started to be evident at 48 h (Fig. 2). Clusters present at 72 h showed an
307 intense fluorescence signal suggesting that these structures were formed by
308 superposition of cellular layers (Fig. 2). From that point onwards, these cellular
309 aggregates became denser and more packed up to 168 h.

310 In G1-B52 samples, significance ($P < 0.05$) corresponding to maximum AVC values
311 were obtained at 24 h of growth ($4.36 \times 10^8 \pm 1.82 \times 10^8$ CFU cm^{-2}) (Fig. 1, Table 3).
312 From that point, AVC outcomes decreased in the following sample times until 96 h

where the minimum AVC value was obtained (about $3.13 \times 10^6 \pm 8.12 \times 10^5$ CFU cm^{-2}) (Fig. 1, Table 3). No statistically significant differences were observed in AVC values between 48 to 168 h (Fig. 1). POA values also displayed similar dynamics where a gradual decrease from 24 h (POA = 30.86 %) until 72 h (POA = 11.64 %) occurred (Fig. 1). Microscopy images gave evidence of cluster formation where high-density groups of red-fluorescent cells were present surrounded by a network of green-fluorescent cells (Fig. 2).

Effectiveness of the sequential application of PRN-BAC on the removal of 168 h L. monocytogenes -E. coli biofilms grown on SS

Different combinations of PRN-BAC were sequentially applied on 168h-old biofilms following a first order factorial design. Quantification of the effects was carried out by combining microscopy and image analysis for occupied area (OA) determination and agar plate count to determine the number of adhered and released viable cultivable cells (AVC and RVC, respectively) after PRN-BAC treatments. In this study, OA will be considered as the main value to obtain the empirical model equation, whereas AVC and RVC outcomes will be used as a supplementary values to determine the actual effects of PRN-BAC solutions.

Occupied area (OA)

Empirical equation [1] significantly ($r^2 = 0{,}927$) described the combined effects of PRN-BAC sequential treatment on the occupied area by undamaged cells (according to LIVE/DEAD staining) in 168 h A1-A14 biofilms:

$$OA\ (mm^2) = 0.46 - 0.12\ \mathbf{BAC} - 0.06\ \mathbf{PRNBAC} \quad [1]$$

Expected OA data according with the equation [1] after the application of PRN-BAC together with several illustrative images are showed in Fig. 3. Additionally, complete statistical data of the model can be found in Table S1.

Statistically significant coefficients in the equation indicated a negative individual effect of BAC against the occupied area by undamaged cells within the biofilm, thus corroborating the effectiveness of BAC as a disinfectant.

No significant effect of the application of PRN alone was demonstrated although the negative interaction PRN-BAC proved an interactive effect of these two components. Whereas the effect of PRN increased the occupied area by undamaged cells of the biofilm at low BAC concentrations, this value was reduced as the enzyme was combined with higher BAC concentrations. Thus, the green signal (undamaged cells) was higher in samples treated at concentrations [1000,50] compared to those treated at [100,50] whereas in the latter a higher red signal was observed (Fig. 3). To check this effect, the experiment was repeated yielding a similar increase in OA value (data not shown). Regardless of OA outcomes, in both experimental points, an altered structure was evident compared to control (Fig. 3). Conversely, at points [100,2000] and [1000,2000] a higher proportion of red (damaged/dead) cells was observed produced by higher BAC concentrations if compared to the aforementioned points. In the latter, large voids with absence of cells were also present pointing out a deep removal of the biofilm caused by the treatment.

The lowest expected value of OA according to equation [1] (46 % respecting to that obtained in absence of treatments) was obtained when PRN and BAC were applied at the highest concentrations. Moreover, at point [1000,2000] the majority of the

360 remaining cells emitted a red fluorescence indicating that those were either damage or
361 dead (Fig. 3).

362

363 *Adhered viable cultivable cells (AVC)*

364 No *L. monocytogenes* A1 AVC from 7-day A1-A14 biofilms were recovered from the
365 coupons after the application of PRN-BAC combinations corresponding to
366 concentrations [100,50], [100,2000], [1000,50] and [1000,2000] μg ml^{-1} (Fig. 4).
367 Conversely, *E. coli* A14 remaining adhered cells were detected in the experimental
368 points where BAC concentrations were low (Fig. 4). Statistical analysis demonstrated
369 that adhered cells of control samples (5.12 ± 0.06 log CFU cm^{-2}) presented significant
370 differences with experimental point [100,50] (4.17 ± 0.05 log CFU cm^{-2}). At high PRN
371 but low BAC concentrations i.e. [1000,50], a higher number of *E. coli* AVC remained
372 attached to the coupon (5.10 ± 0.21 log CFU cm^{-2}). Nonetheless, this value was not
373 significantly different compared to control samples but it did to point [100,50] (Fig. 4).
374 This suggested, together with the outcomes obtained in OA that at low BAC but high
375 PRN concentrations the quantity of biofilm on the coupon increased compared with the
376 other points of the experimental plan (Figs. 3, 4). At points [100,2000] and [1000,2000],
377 *E. coli* A14 AVC counts were below the level of detection thus indicating that the
378 elevated BAC concentrations affected the viability of the remaining attached cells (Fig.
379 4).

380

381 *Released viable cultivable cells (RVC)*

382 No A1 strain RVC from the biofilm were recovered into the neutralising solution after
383 the application of the PRN-BAC treatments as similar as in the adhered cells values.

384 Contrarily, A14 strain RVC were detected in the treatments with low concentration of
385 BAC, i.e. [100,50] and [1000,50] treatments, giving significantly different values of
386 4.90 ± 0.19 and 5.29 ± 0.10 log CFU ml^{-1} at low and high PRN concentration,
387 respectively (Fig. 5), thus indicating that PRN significantly increases *E. coli* cells
388 detachment from the biofilm.

389

390

391

392

393

394

395

396

397

398

399

400

401

402

403

Discussion

Enzymes are considered as good disrupters of biofilm matrices (Meireles et al. 2016). Their combined application with biocides will permit to reduce the doses of disinfectants applied and decrease environmental pollution. Furthermore, characterization of the mixed L. monocytogenes biofilms potentially present on the surfaces of the processing plants would permit to better adjust the cleaning and disinfection protocols applied and consequently, avoid or decrease the generation of resistance.

Quantitative characterisation of two mixed *L. monocytogenes* biofilms were carried out in terms of the number of viable adhered cells and 2D microscopic analysis. 2D areal parameters have been considered as good biofilm descriptors giving biologically meaningful information (Yang et al. 2000; Christensen et al. 2001; Jackson et al. 2001; Beyenal et al. 2004). In our results, fluorescence microscopy analysis provided information regarding 2D structural features not detected by plate count. However, precision of results depends on the uniformity of the structure, giving higher values of coefficient of variation in heterogeneous biofilms (supplementary information). This was of a special relevance in G1-B52 samples in which a clear tendency to form microcolonies was observed (Fig. 2). Microscopic images gave evidence of how these structures were formed by dense groups of red (damaged/dead) cells surrounded by a network of undamaged (green) cells (Fig. 2). Bayles (2007) pointed out the importance of dead cells as a biofilm support, anchoring the whole structure to the surface and thus improving its stability.

The effects of PRN-BAC sequential treatments were assessed on late-stage *L. monocytogenes-E.coli* biofilms using a first-order factorial design. Empirical equation

[1] showed no significance in the individual effects of PRN but indicated a significant individual effect of BAC and an interaction between the effects of PRN and BAC.

PRN is a mixture of various endo- and exo-peptidases (Narahashi 1970). However, although *L. monocytogenes* biofilm matrix has a high protein content (Longhi et al. 2008; Nguyen & Burrows 2014), in all sampling times *L. monocytogenes* A1 population was between 0.35 and 2.16 log CFUcm-2 lower than *E. coli* A14 (Table 2), thus, the contribution for the final matrix composition of A1 strain may be significantly lower if compared with A14 strain. Hence, the absence of individual PRN effect could be related to the presence of soluble protective polysaccharides in the matrix secreted by *E. coli*, becoming richer in sugar residues (Sutherland 2001). Besides, *L. monocytogenes* could have also promoted this sugar-rich environment by secreting soluble polysaccharides such as teichoic acids equal to those present in the cell membrane (Brauge et al. 2016).

In order to mimic as much as possible environmental conditions found in industrial premises, treatments were applied at room temperature, lower than its optimal (Kumar et al. 2004), that may have produced a lower activity of the enzyme. Optimal temperatures have been used in previous biofilm-removal studies involving PRN (Inoue et al. 2003; Rodríguez-López et al. 2017) as well as for other protein hydrolases (Longhi et al. 2008; Nguyen & Burrows 2014). Despite this, Orgaz et al., (2007) demonstrated the effectiveness of PRN at 25 ºC against *P. fluorescens* biofilms. However, the concentration of PRN used was about 4 times more than the maximum used in our work. Nevertheless, among microscopy images it was observed that, if compared with controls, biofilm structure was altered by PRN-BAC in all cases independently of BAC concentration used (Fig. 3).

451 At low BAC concentrations, PRN pre-treatment increased the OA occupied by the
452 mixed biofilm ($OA_{[100,50]}$ = 0.51 mm^2; $OA_{[1000,50]}$ = 0.64 mm^2) (Fig. 3). Regarding to
453 viable-and-cultivable cell quantification, an increase in the number of AVC and RVC of
454 *E. coli* when increasing PRN was detected whereas in *L. monocytogenes* neither AVC
455 nor RVC were detected (Figs. 4, 5). This could be due to an intrinsic higher resistance
456 to QACs of *E. coli* as reported for Gram-negatives (Mcdonnell & Russell 1999;
457 Augustin et al. 2004). Nonetheless, as discussed later, since *L. monocytogenes* can enter
458 into a dormant state where cells still remain alive despite they lack on growth on agar
459 plates, its presence cannot be neglected neither its contribution to the OA increase.

460 The unexpected increase of OA and the number AVC of *E. coli* by PRN in presence of
461 low BAC concentrations can be explained by the dispersant effect of the enzyme (Figs.
462 3, 4). Briefly, the enzyme could have provoked cell disaggregation in the biofilm, and
463 the released cells could have subsequently re-adhered during the time of exposition.
464 This hypothesis would explain, by one hand, the observed increase in the occupied area
465 by the re-adherence and, on the other hand, the observed increase in the number of AVC
466 and RVC.

467 BAC interacts with cell membranes promoting disruption of their integrity and cellular
468 content leakage (Buffet-Bataillon et al. 2012; Tezel & Pavlostathis 2015). At high BAC
469 concentrations, results denoted the interactive effects of PRN-BAC. Indeed, minimum
470 values of OA by undamaged cells of the biofilm were obtained at experimental point
471 [1000,2000] of the factorial design, achieving a 54% reduction of the OA by the biofilm
472 compared to control samples (Fig. 3). These results are in agreement with a recent
473 opinion of Meireles et al. (2016), who stated that a combination of enzymes and
474 biocidal agents is desirable to obtain a good biofilm biomass removal.

No AVC or RVC of *L. monocytogenes* or *E. coli* were detected in those experimental points with the highest BAC concentrations (Figs. 4, 5). However, values of occupied area indicated the presence of undamaged cells on the coupon (Fig. 3). Two main reasons can explain the observed discrepancy. Firstly, the lower limit of detection of the microscopic method (1 cell field^{-1}) respecting to the plate count method (1.70 log CFU cm^{-2}), and secondly, the presence of viable but non-cultivable cells (VBNC). In fact, considering that our experimental system consisted of 168 h biofilms that have been exposed to PRN-BAC treatments, it should be expected that in those biofilms the pool of VBNC cells would be significant. In this state cells do not grow *in vitro* and microscopy assays are the only alternative to detect them (Gião & Keevil 2014).

Moreover, it is becoming clear among microbiologists that microbial pathogens survive to environmental stresses by entering into the VBNC state (Oliver 2005; Gião & Keevil 2014). This status is reversible under appropriate stimuli so, undetected pathogens can resuscitate from this dormant state thus entailing several public health concerns (Li et al. 2014). In *L. monocytogenes* this process is multifactorial (Besnard et al. 2002). Indeed, a recent study carried out in biofilms grown in tap water showed that *L. monocytogenes* VBNC state depends not only on the nutrient availability but also on the temperature (Gião & Keevil 2014).

Cell dispersion is an intrinsic process in the life-cycle of any biofilm (Petrova & Sauer 2016). Nevertheless, antimicrobial treatments can promote a high dispersion after its application (Rodríguez-López et al. 2017). This has been considered as a topic of concern since it can facilitate the dissemination of pathogens into the environment becoming a feasible cause of contamination (Meireles et al. 2016; Shen et al. 2016).

The use of a combined protease-based treatment presented in this work could be useful not only in industrial settings but also in different clinical-related environments (Loiselle & Anderson 2003; Thallinger et al. 2013) to avoid biofilm formation and to remove biomass residues to avoid secondary colonisers to further adhere after an antimicrobial treatment (Cordeiro & Werner 2011). Moreover, enzymatic-based treatments have been used to sensitise biofilm so as to adjust the dose of antibiotics (Selan et al. 1993) and antiseptics (Kaplan 2009) needed for treatment of biofilm-colonised medical devices. A recent study conducted by Stiefel et al., (2016) demonstrated that the use of different species-specific enzyme mixtures increased the efficacy of commercially available cleaners to remove biofilms of *Staphylococcus aureus* and *Pseudomonas aeruginosa* potentially present in endoscopes. Besides, once bacteria are removed from the biofilm, pathogenicity factors may also be affected by enzymatic treatments. As an example, Longhi et al., (2008) observed how the infectiveness of planktonic *L. monocytogenes* in Caco-2 cells was significantly reduced after 24 h treatment with 200 U ml^{-1} of serratiopeptidase. This phenomenon demonstrated that despite live cells are dispersed after enzyme contact, they may represent a lower health threat.

Therefore, the main conclusion of this investigation is that it has been empirically demonstrated the additive effects of PRN-BAC combined treatments for removal of late-stage *L. monocytogenes-E. coli* dual-species biofilms grown on stainless steel. This approach is performed in a straightforward manner with a pre-treatment with PRN combined with a sequential application of a single dose of BAC. Besides, at high BAC concentrations the quantity of released viable cells from the biofilm is also significantly diminished thus avoiding potential pathogen spread into the environment.

List of abbreviations

AVC: Adhered viable cultivable cells

BAC: Benzalkonium chloride

OA: Occupied area

POA: Percentage of occupied area

PRN: Pronase

RVC: Released viable cultivable cells

A1: *Listeria monocytogenes* A1

G1: *Listeria monocytogenes* G1

A14: *Escherichia coli* A14

B52: *Pseudomonas fluorescens* B52

Acknowledgements

All authors acknowledge S. Rodriguez, T. Blanco, V. Nimo and A. Carrera (laboratory technicians, IIM-CSIC) for their help throughout the whole study.

Disclosure statement

All results and discussion presented in this article are part of P. Rodríguez-López PhD dissertation in the framework of the Microbiology Doctorate Programme of the Autonomous University of Barcelona.

Funding

This research was financially supported by the Spanish Ministerio de Economía y Competitividad (ENZYMONO, AGL2010-22212-C02-02). P. Rodríguez-López acknowledges the financial support from the FPI programme (Grant number: BES-2011-050544). All authors acknowledge S. Rodríguez and T. Blanco (laboratory technicians, IIM-CSIC) for their help throughout all the study.

563 **References**

564 Abdallah M, Benoliel C, Drider D, Dhulster P, Chihib NE. 2014. Biofilm formation and
565 persistence on abiotic surfaces in the context of food and medical environments. Arch
566 Microbiol. 196:453–472.

567 Allison DG, Ruiz B, Sanjose C, Jaspe A, Gilbert P. 1998. Extracellular products as
568 mediators of the formation and detachment of Pseudomonas fluorescens biofilms.
569 FEMS Microbiol Lett. 167:179–184.

570 Augustin M, Ali-Vehmas T, Atroshi F. 2004. Assessment of enzymatic cleaning agents
571 and disinfectants against bacterial biofilms. J Pharm Pharm Sci. 7:55–64.

572 Bayles KW. 2007. The biological role of death and lysis in biofilm development. Nat
573 Rev Microbiol. 5:721–6.

574 Besnard V, Federighi M, Declerq E, Jugiau F, Cappelier JM. 2002. Environmental and
575 physico-chemical factors induce VBNC state in Listeria monocytogenes. Vet Res.
576 33:359–370.

577 Beyenal H, Lewandowski Z, Harkin G. 2004. Quantifying biofilm structure: facts and
578 fiction. Biofouling. 20:1–23.

579 Box GEP. 1952. Multi-Factor Designs of First Order. Biometrika. 39:49–57.

580 Box GEP, Hunter WG, Hunter JS. 2008. Diseños factoriales y transformación de datos.
581 In: Estadística para Investig Diseño, innovación y Descub (2nd Ed. 2nd ed. [place
582 unknown]: Ed. Reverté.

583 Brauge T, Sadovskaya I, Faille C, Benezech T, Maes E, Guerardel Y, Midelet-Bourdin
584 G. 2016. Teichoic acid is the major polysaccharide present in the Listeria

585 monocytogenes biofilm matrix. FEMS Microbiol Lett. 363:fnv229.

586 Bridier a, Briandet R, Thomas V, Dubois-Brissonnet F. 2011. Resistance of bacterial
587 biofilms to disinfectants: a review. Biofouling. 27:1017–32.

588 Bridier A, Sanchez-Vizuete P, Guilbaud M, Piard JC, Naïtali M, Briandet R. 2015.
589 Biofilm-associated persistence of food-borne pathogens. Food Microbiol. 45:167–178.

590 Buffet-Bataillon S, Tattevin P, Bonnaure-Mallet M, Jolivet-Gougeon A. 2012.
591 Emergence of resistance to antibacterial agents: The role of quaternary ammonium
592 compounds - A critical review. Int J Antimicrob Agents. 39:381–389.

593 Carpentier B, Cerf O. 2011. Review - Persistence of Listeria monocytogenes in food
594 industry equipment and premises. Int J Food Microbiol. 145:1–8.

595 Carpentier B, Chassaing D. 2004. Interactions in biofilms between Listeria
596 monocytogenes and resident microorganisms from food industry premises. Int J Food
597 Microbiol. 97:111–22.

598 Christensen BE, Ertesvag H, Beyenal H, Lewandowski Z. 2001. Resistance of biofilms
599 containing alginate-producing bacteria to disintegration by an alginate degrading
600 enzyme (Algl). Biofouling. 17:203–210.

601 Cordeiro AL, Werner C. 2011. Enzymes for Antifouling Strategies. J Adhes Sci
602 Technol. 25:2317–2344.

603 Costerton JW, Lewandowski Z, Caldwell DE, Korber DR, Lappin-Scott HM. 1995.
604 Microbial biofilms. Annu Rev Microbiol. 49:711–745.

605 Davey ME, O'toole GA. 2000. Microbial biofilms: from ecology to molecular genetics.
606 Microbiol Mol Biol Rev. 64:847–67.

607 Dusane DH, Rajput JK, Kumar AR, Nancharaiah Y V, Venugopalan VP, Zinjarde SS.
608 2008. Disruption of fungal and bacterial biofilms by lauroyl glucose. Lett Appl
609 Microbiol. 47:374–9.

610 EFSA. 2015. The European Union summary report on trends and sources of zoonoses,
611 zoonotic agents and food-borne outbreaks in 2014. EFSA J. 13:4329.

612 Freitag NE, Port GC, Miner MD. 2009. Listeria monocytogenes - from saprophyte to
613 intracellular pathogen. Nat Rev Microbiol. 7:623–8.

614 Gandhi M, Chikindas ML. 2007. Listeria: A foodborne pathogen that knows how to
615 survive. Int J Food Microbiol. 113:1–15.

616 Gião MS, Keevil CW. 2014. Listeria monocytogenes can form biofilms in tap water and
617 enter into the viable but non-cultivable state. Microb Ecol. 67:603–11.

618 Giaouris E, Chorianopoulos N, Doulgeraki A, Nychas G-J. 2013. Co-culture with
619 Listeria monocytogenes within a dual-species biofilm community strongly increases
620 resistance of Pseudomonas putida to benzalkonium chloride. PLoS One. 8:e77276.

621 Houari A, Di Martino P. 2007. Effect of chlorhexidine and benzalkonium chloride on
622 bacterial biofilm formation. Lett Appl Microbiol. 45:652–6.

623 Inoue T, Shingaki R, Sogawa N, Sogawa CA, Asaumi J, Kokeguchi S, Fukui K. 2003.
624 Biofilm formation by a fimbriae-deficient mutant of Actinobacillus
625 actinomycetemcomitans. Microbiol Immunol. 47:877–881.

626 Jackson G, Beyenal H, Rees WM, Lewandowski Z. 2001. Growing reproducible
627 biofilms with respect to structure and viable cell counts. J Microbiol Methods. 47:1–10.

628 Kaplan JB. 2009. Therapeutic potential of biofilm-dispersing enzymes. Int J Artif

629 Organs. 32:545–554.

630 Kaplan JB. 2014. Biofilm matrix-degrading enzymes. Methods Mol Biol. 1147:203–13.

631 Kostaki M, Chorianopoulos N, Braxou E, Nychas G-J, Giaouris E. 2012. Differential
632 biofilm formation and chemical disinfection resistance of sessile cells of listeria
633 monocytogenes strains under monospecies and dual-species (with Salmonella enterica)
634 conditions. Appl Environ Microbiol. 78:2586–95.

635 Kumar ABV, Gowda LR, Tharanathan RN. 2004. Non-specific depolymerization of
636 chitosan by pronase and characterization of the resultant products. Eur J Biochem.
637 271:713–723.

638 Leite P, Rodrigues R, Ferreira M, Ribeiro G, Jacquet C, Martin P, Brito L. 2006.
639 Comparative characterization of Listeria monocytogenes isolated from Portuguese
640 farmhouse ewe's cheese and from humans. Int J Food Microbiol. 106:111–21.

641 Lequette Y, Boels G, Clarisse M, Faille C. 2010. Using enzymes to remove biofilms of
642 bacterial isolates sampled in the food-industry. Biofouling. 26:421–31.

643 Li L, Mendis N, Trigui H, Oliver JD, Faucher SP. 2014. The importance of the viable
644 but non-culturable state in human bacterial pathogens. Front Microbiol. 5:1–1.

645 Loiselle M, Anderson KW. 2003. The use of cellulase in inhibiting biofilm formation
646 from organisms commonly found on medical implants. Biofouling. 19:77–85.

647 Longhi C, Scoarughi GL, Poggiali F, Cellini A, Carpentieri A, Seganti L, Pucci P,
648 Amoresano A, Cocconcelli PS, Artini M, et al. 2008. Protease treatment affects both
649 invasion ability and biofilm formation in Listeria monocytogenes. Microb Pathog.
650 45:45–52.

651 Marion K, Freney J, James G, Bergeron E, Renaud FNR, Costerton JW. 2006. Using an
652 efficient biofilm detaching agent: an essential step for the improvement of endoscope
653 reprocessing protocols. J Hosp Infect. 64:136–142.

654 McCarthy S, Burkhardt W. 2012. Efficacy of electrolyzed oxidizing water against
655 Listeria monocytogenes and Morganella morganii on conveyor belt and raw fish
656 surfaces. Food Control. 24:214–219.

657 Mcdonnell G, Russell AD. 1999. Antiseptics and disinfectants: Activity, action, and
658 resistance. Clin Microbiol Rev. 12:147–179.

659 Meireles A, Borges A, Giaouris E, Simões M. 2016. The current knowledge on the
660 application of anti-biofilm enzymes in the food industry. Food Res Int. 86:140–146.

661 Muhterem-Uyar M, Dalmasso M, Bolocan AS, Hernandez M, Kapetanakou AE, Kuchta
662 T, Manios SG, Melero B, Minarovičová J, Nicolau AI, et al. 2015. Environmental
663 sampling for Listeria monocytogenes control in food processing facilities reveals three
664 contamination scenarios. Food Control. 51:94–107.

665 Narahashi Y. 1970. Pronase. Methods Enzymol. 19:651–664.

666 Nguyen UT, Burrows LL. 2014. DNase I and proteinase K impair Listeria
667 monocytogenes biofilm formation and induce dispersal of pre-existing biofilms. Int J
668 Food Microbiol. 187:26–32.

669 O'Toole G, Kaplan HB, Kolter R. 2000. Biofilm formation as microbial development.
670 Annu Rev Microbiol. 54:49–79.

671 Oliver JD. 2005. The viable but nonculturable state in bacteria. J Microbiol. 43:93–100.

672 Orgaz B, Neufeld RJ, SanJose C. 2007. Single-step biofilm removal with delayed

673 release encapsulated Pronase mixed with soluble enzymes. Enzyme Microb Technol.
674 40:1045–1051.

675 Petrova OE, Sauer K. 2016. Escaping the biofilm in more than one way: Desorption,
676 detachment or dispersion. Curr Opin Microbiol. 30:67–78.

677 Rodríguez-López P, Carballo-Justo A, Draper LA, Cabo ML. 2017. Removal of Listeria
678 monocytogenes dual-species biofilms using enzyme-benzalkonium chloride combined
679 treatments. Biofouling. 33:45–58.

680 Rodríguez-López P, Saá-Ibusquiza P, Mosquera-Fernández M, López-Cabo M. 2015.
681 Listeria monocytogenes – carrying consortia in food industry. Composition, subtyping
682 and numerical characterisation of mono-species biofilm dynamics on stainless steel. Int
683 J Food Microbiol. 206:84–95.

684 Saá Ibusquiza P, Herrera JJR, Cabo ML. 2011. Resistance to benzalkonium chloride,
685 peracetic acid and nisin during formation of mature biofilms by Listeria
686 monocytogenes. Food Microbiol. 28:418–25.

687 Selan L, Berlutti F, Passariello C, Berlutii F, Comodi-ballanti MR, Thaller MC. 1993.
688 Proteolytic enzymes : a new treatment strategy for prosthetic infections ? Proteolytic
689 Enzymes : a New Treatment Strategy for Prosthetic Infections ? Antimicrob Agents
690 Chemother. 37:2618–2621.

691 Shen Y, Huang C, Monroy GL, Janjaroen D, Derlon N, Lin J, Espinosa-Marzal R,
692 Morgenroth E, Boppart SA, Ashbolt NJ, et al. 2016. Response of Simulated Drinking
693 Water Biofilm Mechanical and Structural Properties to Long-Term Disinfectant
694 Exposure. Environ Sci Technol. 50:1779–1787.

695 da Silva EP, De Martinis ECP. 2013. Current knowledge and perspectives on biofilm

696 formation: the case of Listeria monocytogenes. Appl Microbiol Biotechnol. 97:957–68.

697 Stiefel P, Mauerhofer S, Schneider J, Maniura-Weber K, Rosenberg U, Ren Q. 2016.
698 Enzymes enhance biofilm removal efficiency of cleaners. Antimicrob Agents
699 Chemother. 60:3647–3652.

700 Sutherland IW. 2001. Microbial polysaccharides from Gram-negative bacteria. Int Dairy
701 J. 11:663–674.

702 Sutton S. 2011. Accuracy of plate counts. J Valid Technol. 17:42–46.

703 Tezel U, Pavlostathis SG. 2015. Quaternary ammonium disinfectants: microbial
704 adaptation, degradation and ecology. Curr Opin Biotechnol. 33:296–304.

705 Thallinger B, Prasetyo EN, Nyanhongo GS, Guebitz GM. 2013. Antimicrobial
706 enzymes: an emerging strategy to fight microbes and microbial biofilms. Biotechnol J.
707 8:97–109.

708 Vázquez-Sánchez D, Cabo ML, Rodríguez-Herrera JJ. 2014. Single and Sequential
709 Application of Electrolyzed Water with Benzalkonium Chloride or Peracetic Acid for
710 Removal of Staphylococcus Aureus Biofilms. J Food Saf. 34:199–210.

711 Vlamakis H. 2011. The world of biofilms. Virulence. 2:431–434.

712 Winkelströter LK, Teixeira FB dos R, Silva EP, Alves VF, De Martinis ECP. 2013.
713 Unraveling Microbial Biofilms of Importance for Food Microbiology. Microb Ecol.
714 68:35–46.

715 Yang X, Beyenal H, Harkin G, Lewandowski Z. 2000. Quantifying biofilm structure
716 using image analysis. J Microbiol Methods. 39:109–119.

717 Zhang J, Cao G, Xu X, Allard M, Li P, Brown E, Yang X, Pan H, Meng J. 2016.

718 Evolution and Diversity of Listeria monocytogenes from Clinical and Food Samples in
719 Shanghai, China. Front Microbiol. 7:1138.

720

721

722

723

724

725

726

727

728

729

730

731

732

733

734

735

736

737 **Figures**

738

739

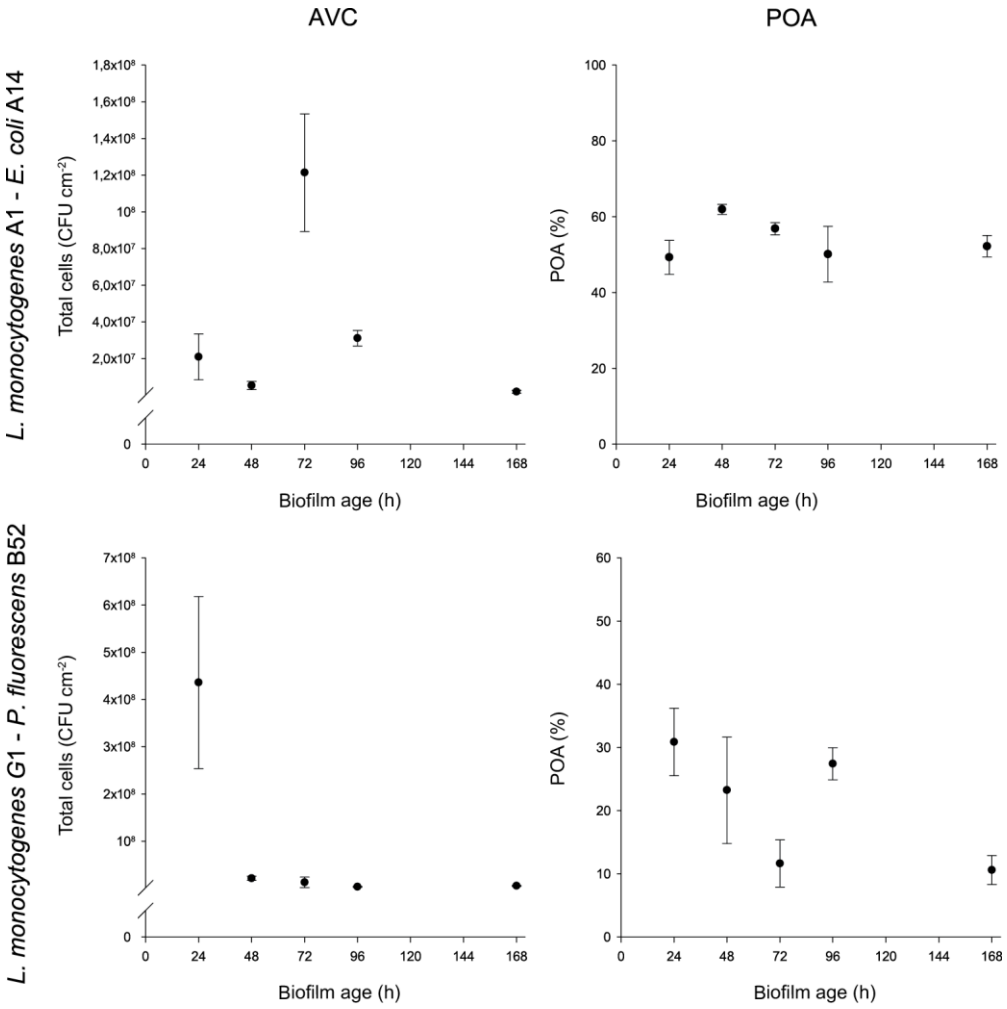

740

741 **Figure 1.** Representation of total number of attached viable cultivable cells (AVC) and
742 percentage of occupied area (POA) values of fish and dairy industry consortia obtained
743 in biofilm formation kinetics. Error bars represent SD values (n = 3, for each assay).

744

745

746

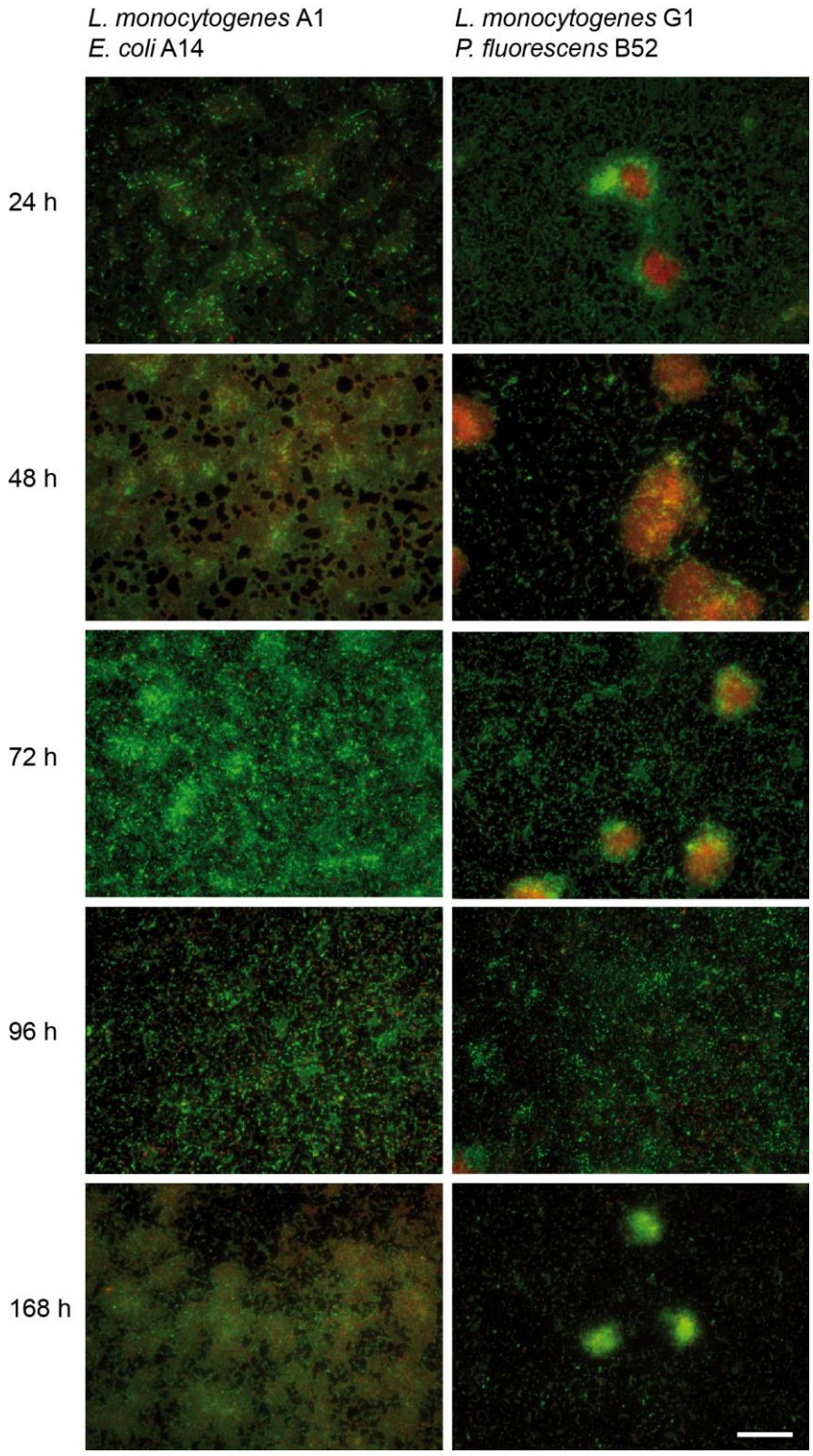

747

748 **Figure 2.** Formation kinetics of *Listeria monocytogenes* dual-species biofilms.
749 Fluorescence microscope 40x-field images obtained after LIVE/DEAD staining. Green
750 cells represent undamaged (live) cells whereas red cells represent either damaged or
751 dead cells (Scale bar = 50 µm).

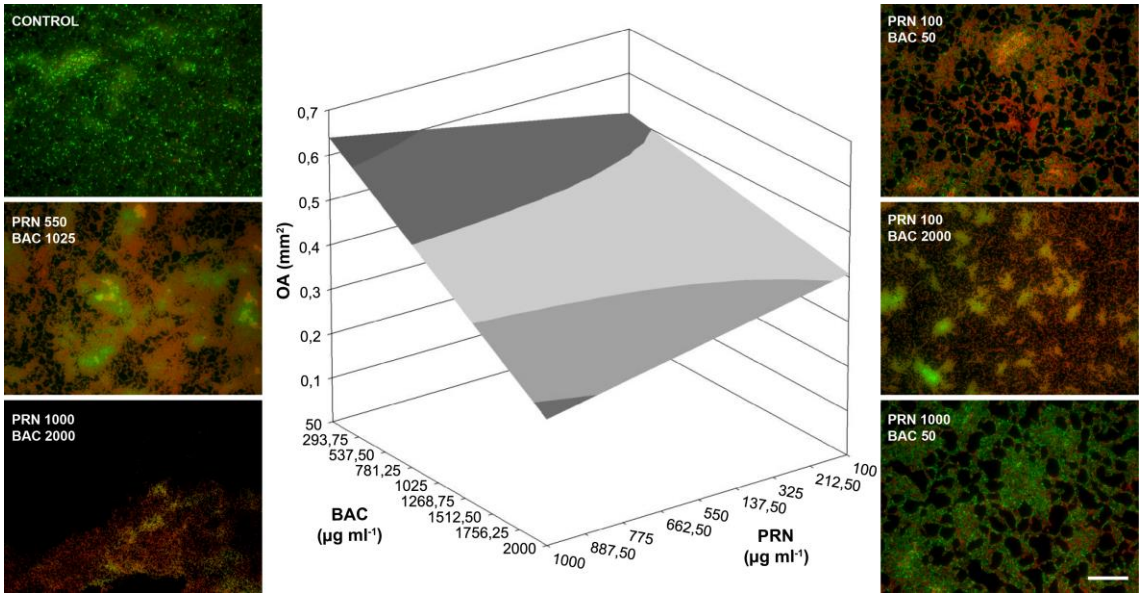

Figure 3. Central: Values of occupied area (OA) expressed in mm^2 after the combined sequential application of pronase (PRN) and benzalkonium chloride (BAC) on 168 h *Listeria monocytogenes* A1-*Escherichia coli* A14 biofilms. Sides: Representative epifluorescence 40x field images of control and PRN-BAC treated samples stained with LIVE/DEAD staining (Scale bar = 50 µm). Numbers in each image indicate the concentration used of each component, expressed in µg ml^{-1}.

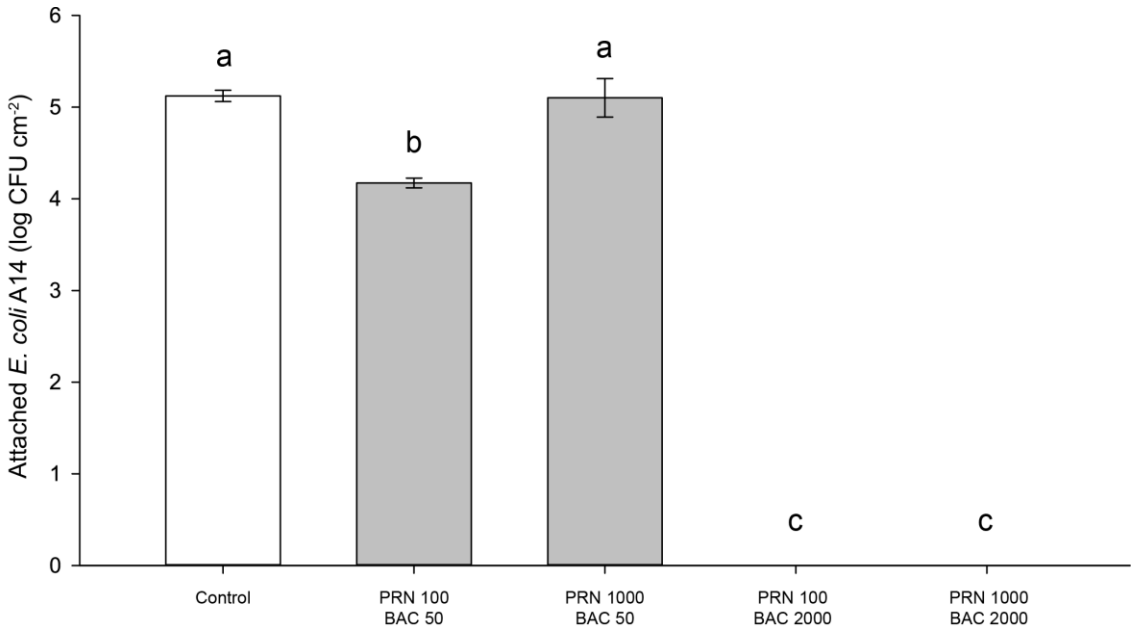

Figure 4. Remaining viable *Escherichia coli* A14 attached cells after the sequential application of different solutions of pronase (PRN) followed by a dose of benzalkonium chloride (BAC) on 168 h *L. monocytogenes* A1-*Escherichia coli* A14 biofilms. Values in x axis indicate the concentrations used of each component, expressed in μg ml^{-1}. Error bars represent SD values (n = 3). Different letters indicate statistical significance (one-way ANOVA, $\alpha = 0.05$).

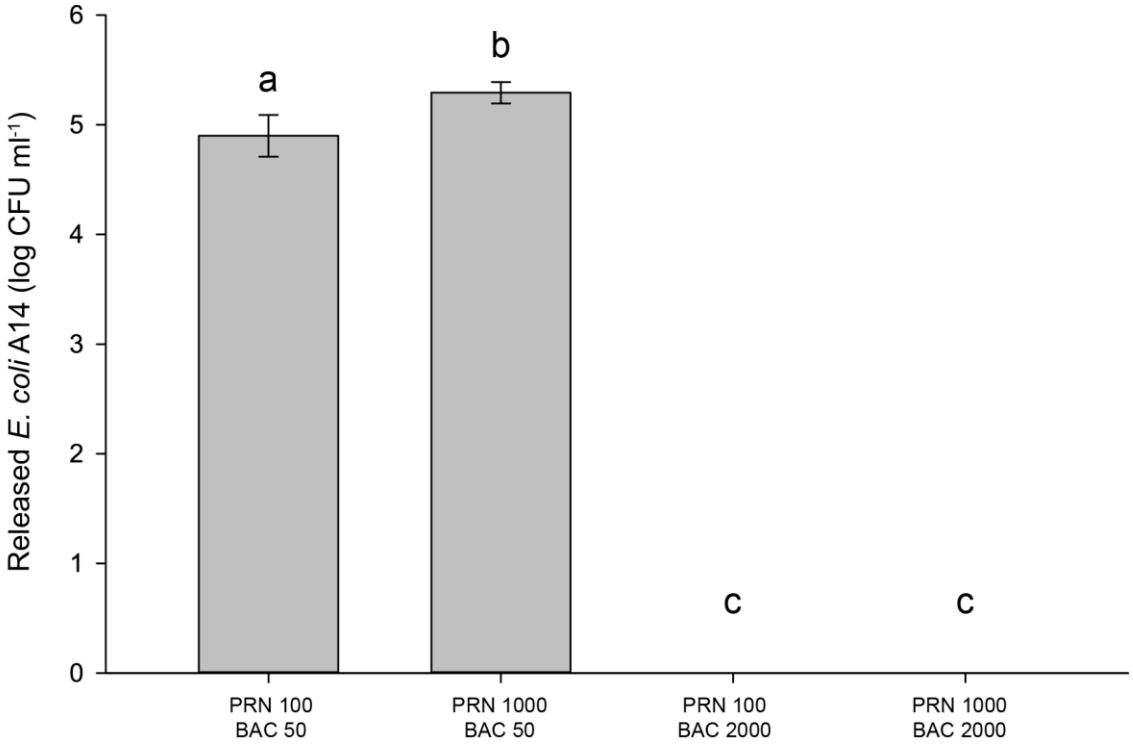

Figure 5. Viable *Escherichia coli* A14 cells recovered from the neutralising solution after sequential application of pronase (PRN) followed by a benzalkonium chloride (BAC) dose on 168 h *L. monocytogenes* A1-*Escherichia coli* A14 biofilms. Values in x axis indicate the concentrations used of each component, expressed in μg ml^{-1}. Error bars represent SD values (n = 3). Different letters indicate statistical significance (one-way ANOVA, $\alpha = 0.05$)**.**

Tables

Table 1. Natural and encoded values corresponding to the concentrations of pronase (PRN) and benzalkonium chloride (BAC) used in the first-order factorial approach followed in this study.

Encoded values	Natural values	
	PRN (µg ml^{-1})	BAC (µg ml^{-1})
[-1,-1]	100	50
[-1,1]	100	2000
[1,-1]	1000	50
[1,1]	1000	2000
[0,0]	550	1025
[0,0]	550	1025
[0,0]	550	1025
[0,0]	550	1025

807 **Table 2.** AVC mean values (n = 3) in CFU cm^{-2} and standard deviations (SD)
808 corresponding to the growth kinetics of *L. monocytogenes* A1 – *E. coli* A14 dual-
809 species biofilm on stainless steel.

810

	L. monocytogenes A1		*E. coli* A14		Total cells	
Age (h)	**Mean**	**SD**	**Mean**	**SD**	**Mean**	**SD**
24	$7{,}07 \times 10^{6}$	$5{,}88 \times 10^{6}$	$1{,}38 \times 10^{7}$	$7{,}08 \times 10^{6}$	$2{,}09 \times 10^{7}$	$1{,}25 \times 10^{7}$
48	$1{,}19 \times 10^{6}$	$3{,}24 \times 10^{5}$	$4{,}14 \times 10^{6}$	$2{,}29 \times 10^{6}$	$5{,}32 \times 10^{6}$	$2{,}25 \times 10^{6}$
72	$8{,}33 \times 10^{5}$	$2{,}63 \times 10^{5}$	$1{,}21 \times 10^{8}$	$3{,}21 \times 10^{7}$	$1{,}21 \times 10^{8}$	$3{,}20 \times 10^{7}$
96	$1{,}50 \times 10^{6}$	$1{,}70 \times 10^{5}$	$2{,}96 \times 10^{7}$	$2{,}82 \times 10^{6}$	$3{,}11 \times 10^{7}$	$2{,}99 \times 10^{6}$
168	$5{,}13 \times 10^{5}$	$2{,}32 \times 10^{5}$	$1{,}40 \times 10^{6}$	$6{,}84 \times 10^{5}$	$1{,}91 \times 10^{6}$	$8{,}44 \times 10^{5}$

811
812
813
814
815
816
817
818
819
820
821
822

Table 3. AVC mean values (n = 3) in CFU cm^{-2} and standard deviations (SD) corresponding to the growth kinetics of *L. monocytogenes* G1 – *P. fluorescens* B52 dual-species biofilm on stainless steel.

	L. monocytogenes G1		*P. fluorescens* B52		Total cells	
Age (h)	**Mean**	**SD**	**Mean**	**SD**	**Mean**	**SD**
24	$6{,}59 \times 10^{7}$	$2{,}30 \times 10^{7}$	$3{,}70 \times 10^{8}$	$1{,}76 \times 10^{8}$	$4{,}36 \times 10^{8}$	$1{,}82 \times 10^{8}$
48	$6{,}06 \times 10^{6}$	$2{,}73 \times 10^{6}$	$1{,}52 \times 10^{7}$	$7{,}00 \times 10^{6}$	$2{,}13 \times 10^{7}$	$4{,}29 \times 10^{6}$
72	$3{,}90 \times 10^{6}$	$2{,}74 \times 10^{6}$	$8{,}81 \times 10^{6}$	$8{,}66 \times 10^{6}$	$1{,}27 \times 10^{7}$	$1{,}13 \times 10^{7}$
96	$1{,}49 \times 10^{6}$	$4{,}46 \times 10^{5}$	$1{,}65 \times 10^{6}$	$6{,}64 \times 10^{5}$	$3{,}13 \times 10^{6}$	$8{,}12 \times 10^{5}$
168	$3{,}23 \times 10^{5}$	$1{,}43 \times 10^{5}$	$4{,}85 \times 10^{6}$	$1{,}25 \times 10^{6}$	$5{,}18 \times 10^{6}$	$1{,}18 \times 10^{6}$

Supplementary information

Repeatability and reproducibility of occupied area (OA) and agar plate count assays in quantification of Listeria monocytogenes mixed-species biofilm formation

Repeatability, defined as the ability of a particular method to generate the same outcomes over a short period of time under the same conditions (Synder et al. 2010), was obtained by calculating the intra-assay variation among images (3x25-field mosaics) and plate counts of 9 different coupons of *L. monocytogenes* A1-*Escherichia coli* A14 and *L. monocytogenes* G1-*Pseudomonas fluorescens* B52 samples harvested at 24 and 168 h.

Obtained results showed that in both consortia data dispersion was larger in attached viable cultivable cells (AVC) values compared with OA (Fig. S1). If each consortium is individually compared, AVC dispersion was higher in A1-A14 whereas in OA, G1-B52 samples presented less dispersed values. In all cases, interquartile range (IQR) values regarding agar plating gave higher values compared to those obtained in OA determinations. So, OA determination could be considered repeatable when comparing with the determination of the number of adhered cells by the classical method of swabbing and plate count.

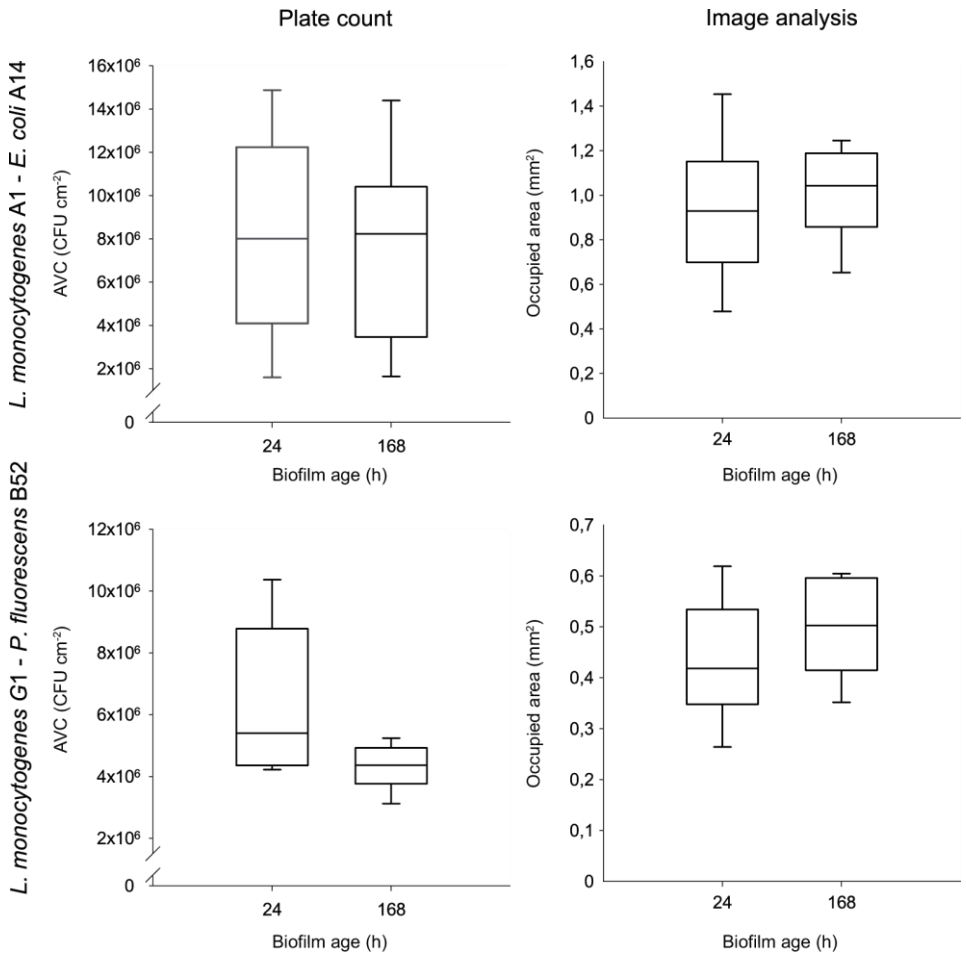

855

856 **Figure S1.** Boxplot and whiskers diagrams showing the distribution of values obtained in repeatability
857 assays in fish and dairy industry consortia (n = 9). Bottom, middle and top lines represent Q1, median and
858 Q3, respectively.

859

860 Reproducibility is defined as the variation values obtained among analysts (Synder et al.
861 2010). In an initial phase, it was obtained by comparing the values of the occupied area
862 by the undamaged cells of a 24 h A1-A14 biofilm calculated by 3 analysts with different
863 level of expertise in microscopy and image analysis (Fig. S2). Analyst 1 was a
864 technician who had performed some image analyses previously, analyst 2 an
865 experienced technician and analyst 3 an untrained technician with basic knowledge in
866 microscopy image analysis.

Results showed that OA values obtained by analyst 2 were significantly higher than those obtained by analysts 1 and 3. Besides, it was observed that outcomes obtained by analyst 3 presented the highest dispersion. In a second phase, analyst 3 was in-house trained by analyst 2 in image analysis during a period of about a month. OA values of the same images set were re-calculated by analyst 2 and outcomes were compared again. As observed in Fig. 2, values of occupied area obtained after training were not significantly different to those obtained by analyst 2 although a high dispersion was still observed.

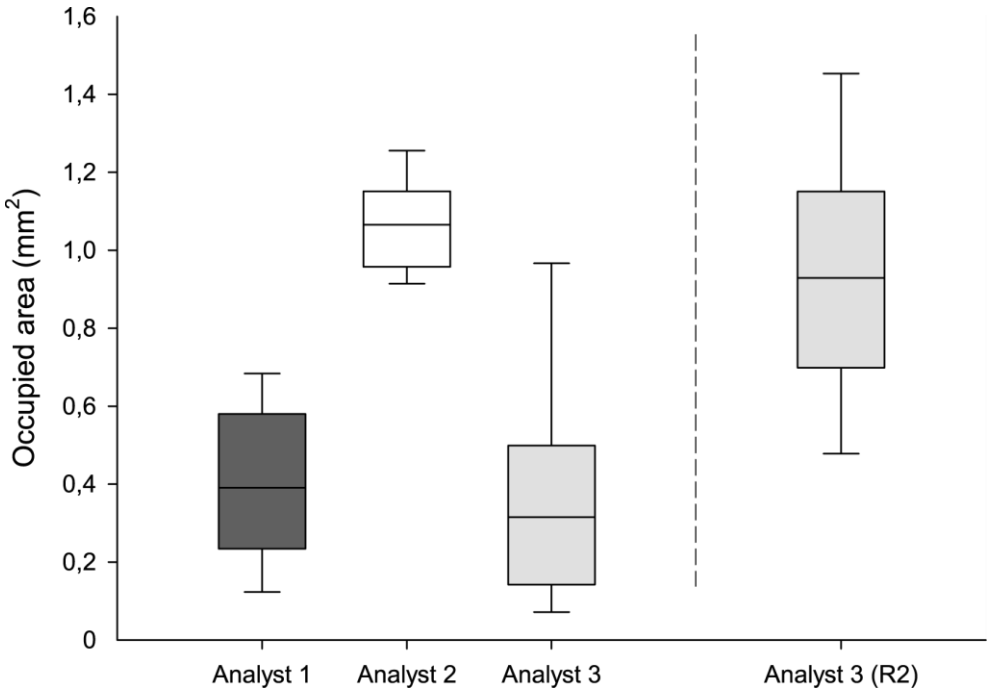

Figure S2. Boxplot and whiskers diagrams showing the distribution of values obtained by different analysts in reproducibility assays (n = 9). Box named as *Analyst 3 (R2)* corresponds to the values obtained by analyst 3 after in-house training.

Precision of plate count and microscopy image analysis in the assessment of biofilm formation kinetics in L. monocytogenes dual-species biofilms

Precision of both methods was evaluated by comparing the coefficients of variation (CV) of the values of AVC obtained by plate count and POA obtained by image analysis (Fig. S3). Taking as a reference the quantitation limit in analytical chemistry, a CV value ≤ 20% was considered as acceptable measurements whereas a value > 20% was considered as low precision values which can only be used with descriptive purposes (Mark Green 1996).

Generally, acceptable CV values were obtained in occupied area when analysing fish and dairy consortia. More specifically, results of POA in A1-A14 samples rendered CV values below 10 % in all experimental times except at 96 h (21.17 %). In plate count, CV values were above 20 % in all sample times but at 96 h (13.55%) (Fig. S3). In G1-B52 biofilms, CV values obtained in POA were around 20 % at 24, 48 and 168 h whereas in plate count, CV values were all above 20 % excepting at 96 h. Besides, even though above the threshold, CV value at 168 h was still around the threshold value (Fig. S3).

Taking all these results together indicate that, numerically, the occupied area can be considered a reliable 2D-structural parameter to quantify the dynamics of *L. monocytogenes* dual-species biofilm formation. Besides, it provides easy-to-interpret biological information regarding morphology and distribution of the biofilm along the surface.

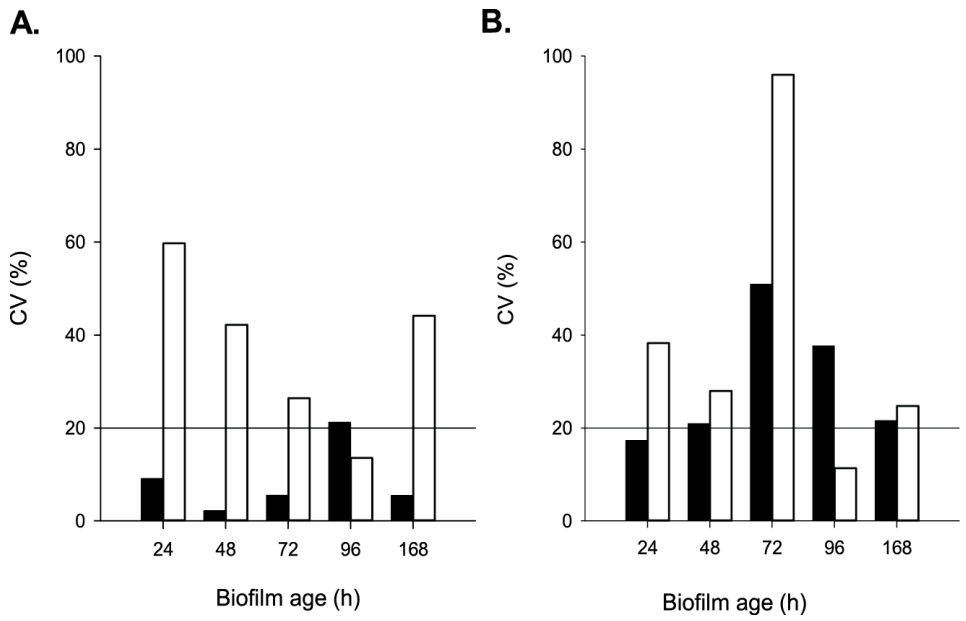

905

906 **Figure S3.** Coefficients of variation of fish (A) and dairy (B) industry consortia obtained with image

907 analysis (■) and plate count (☐) (n = 3, for each assay).

908

909

910

911

912

913

914

915

916

917

918

Table S1. Effects of PRN and BAC treatments on the occupied area (OA) in mm^2 on 168 h *L. monocytogenes* A1-*E. coli* A14 biofilms. Results of factorial design and test of significance for model in equation [1].

PRN	BAC	OA_{obs}	OA_{exp}	Coefficients	t	Model
1	1	0.258	0.28	0.46	35.00	0.46
1	-1	0.617	0.64	-0.02	0.94	-
-1	1	0.421	0.41	-0.12	6.24	-0.12 BAC
-1	-1	0.525	0.51	-0.06	3.44	-0.06 PRNBAC
0	0	0.440	0.46	Average value =		3.673
0	0	0.414	0.46	Expected average value =		3.67
0	0	0.510	0.46	Var (Ee) =		0.0014
0	0	0.428	0.46	t (α = 0.05; υ = 3) =		3.182

	SS	υ	MS				
				MSM/MSE =	31.943	F 0.05 {2;5} =	5.786
Model	0.070	2	0.035	MSMLF/MSM =	0.510	F 0.05 {4;2} =	19.247
Error	0.005	5	0.001	MSE/MSEe =	0.795	F 0.05 {5;3} =	9.117
Experimental error	0.004	3	0.001	MSLF/MSEe =	0.487	F 0.05 {2;3} =	9.552
Lack of fitting	0.001	2	0.001	r^2 =	0.927		
Total	0.075	7	0.011	Corrected r^2 =	0.898		

MSM: minimum squares model; **MSE**: Minimum squares error; **MSMLF**: Minimum squares model lack of fitting; **MSEe**: Minimum squares experimental error

930 **References**

931 Mark Green J. 1996. A practical guide to analytical method validation. Anal Chem.
932 68:305A–309A.

933 Synder LR, Kirkland JJ, Doland JW. 2010. Method Validation. In: Synder LR, Kirkland
934 JJ, Dolan JW, editors. Introd to Mod Liq Chromatogr. 3rd ed. New York, NY: John
935 Wiley & Sons, Inc.; p. 531–567.

936

937